

Magnetic Shielding In a Cryogenic Environment

by Robert F. Arentz and Mark H. Johnson, Ball Aerospace Systems Division, Boulder, CO, and Lester Dant, Ad-Vance Magnetics, Inc., Rochester, IN (219) 223-3158

A report on the changes in the magnetic shielding efficiency of a commercially available, high permeability material as a function of fabrication, annealing process, temperature, field intensity and frequency is presented. Data are presented for the same alloy treated by two different processes. Data were taken at 300°, 77°, 4° and 1.91°K, with sinusoidal excitation field strengths of 5 and 50 gauss. One of the samples remained stable above 1 kHz and, in fact, showed an improvement in its shielding efficiency at 4°K over that at 300°K. The other sample showed significant shielding degradation at 4°K at these high frequencies. Because of the relatively stable behavior of both materials as a function of temperature at low frequencies, they would, therefore, be useful for localized, cryogenically cooled magnetic shielding in such systems as SQUIDS, satellite-borne magnetometers and particle detectors.

Our involvement with cryogenically cooled magnetic shielding began with a need to design a shield for a spaceborne, superfluid-cooled SQUID-based, magnetometer system known as the Stanford Relativity Experiment or GP-B.

At that time, useful and cryogenically stable shielding materials were completely unknown to us. A material called Cryoperm-10¹ was called to our attention by the Electromagnetic Technology Division of the National Bureau of Standards. This material has been measured at 4.4°K to have an initial permeability of 8.81×10^{-2} H.m (70,000 μ), and a maximum permeability of 3.14×10^{-1} (250,000 μ). Even though this material has good magnetic properties, it was eventually dropped from consideration for several reasons having to do, in part, with the difficulties involved with purchasing, MIL-Spec certification and a maximum strip width.

Our search produced only five references dealing directly with the measurements of the shielding factor or permeability characteristics of ferromagnetic alloys at low field strengths ($.6 \times 10^{-4}$ T), low temperatures (1.9° to 4°K) and low frequencies (.01 to 10 kHz); and one reference dealing with all of these for pure iron.

We agree completely with Suzuki et al., "that the performance of ferromagnetic shields immersed directly in liquid helium has rarely been reported."

In the five references cited, one finds a regular bestiary of materials identified only by their trade names; but few references for alloy composition or sources. Furthermore, a property such as permeability is often quoted only as a ratio between two temperatures, but the absolute permeability is left unstated. Also data are not usually taken over a broad range of frequencies.

As will be seen in our data curves, large differences do occur over a relatively short frequency span, particularly in the decade between 100 and 1 kHz. In addition, each reference

cites at least one anecdotal contribution to unusual magnetic characteristics such as strain, annealing at high temperatures, cooling and annealing profiles below 100°K, applied field strengths and alloy purity. To compound the confusion, some works measure properties that are temperature independent, such as saturation induction (B_s). Some measure initial permeability, some measure maximum permeability which are nearly impossible to compare and a few measure the actual B-H curve.

There is a multitude of magnetic shielding alloys available in today's marketplace, each alloy having its own individual distinct characteristics. There are various formulations ranging from industry standards to exotic concoctions, each having its own magnetic properties, physical properties and shielding effectiveness sensitive to frequency, temperature and magnetic environment.

Identification of a specific alloy may be revealed by a military specification, a manufacturer's published specification or a fabricator's-seller's trade name.

Optimum magnetic shielding for a specific application is a result of many factors, including:

- The proper selection of alloy chemistry.
- Good metallurgical mill practice.
- Thickness of material.
- Physical size and configuration.
- Technique of fabrication.
- Final annealing process.

Nearly all magnetic measurements are difficult to make, let alone when added to the problems of a cryogenic magnetics measurement. We, therefore, chose to measure the shielding factor of an enclosed, right circular cylinder, that was 17.8 cm high, 7.62 cm wide (OD) and with a wall thickness of 1 mm. The material we tested is an alloy called AD-MU-78.

AD-MU-78 is a high permeability, ferromagnetically soft alloy with a nominal composition by weight percentage of Ni (75-77), Fe (12-15), Cu (4-6) and a maximum content of Cr (3), Mg (1.8), Si (0.5), Ph (0.02), S (0.02) and C (0.05). We received two cans with end caps for study. Although the two specimens were made from the same ingot of material, they had undergone separate and distinct processes. Can No. 1 (henceforth called AD-MU-78) underwent a standard processing used by the manufacturer. Can No. 2 (henceforth called CP-EXP-1184) underwent a proprietary processing. Both cans were formed by a heliarced, butt-weld seam along their longitudinal axis and by a welded plate for the bottom. The end caps slipped tightly over the outer walls of the cylinder with a 2 cm overlap. In the center of each cap, there was a .64 cm dia hole through which leads for the pickup coil

could be routed, and cryogenic fluids could fill the interior volume.

All in all, we found the alloy to be very tractable from all points of view. It forms and welds easily. It can be purchased in sheets up to 40.6 cm wide and in lengths up to 3 meters long. It comes in a variety of thicknesses. Its alloy composition is well documented and can be purchased to a MIL-Spec (MIL-N-14411, Composition 2). It is made in the U.S. and interacting with the manufacturer is very easy. Its price is competitive, and its magnetic properties are quite good.

Experimental Procedure

Our setup was quite simple and standard. We drove a controlled, sinusoidal current into a pair of coils hooked in series-aiding and measured the induced, open-circuit output voltages of a third coil located between them.

The geometry of the three coils was always fixed and the coupling between the coils was measured first without, and then with the can inserted between the coils.

The shielding factor is then simply the ratio of the two signal levels. We varied the drive frequency continuously over the range of .008 Hz to 12 kHz, and selected two rms drive currents of 20 mA and 160 mA. These currents gave us fields which maximum rms values were 4 and 50 gauss at the contact interface between a drive coil and the wall of the can. These field levels were measured with a calibrated, thin Hall-effect sensor probe carefully inserted between the coil and the surface.

Due to our selection of available instrumentation, we chose to monitor the input rms current on a calibrated John Fluke 850LA meter; and to measure the output voltage signal on a calibrated Hewlett-Packard 3582A spectrum analyzer. Our exact set-up is depicted in Figure 1. Note that the entire system is dc coupled.

Since our test configuration converted an input rms current into an output rms voltage, our transfer function is dimensionally that of transconductance. Since we can't think very clearly in mhos, we have chosen to invert our numbers to ohms by dividing the output voltage by the input current.

Having the input coil inside the can reduced our 60 Hz pickup to virtually nothing. We added a hand-built, two-stage preamp in the pick-up line directly at the output from the dewar. This gave us a dc offset control to compensate for thermal drifts in the Ithaco instrumentation amplifier which was run at fixed and measured gains between 1,000 and 10,000. The two-stage preamp was built up from Precision Monolithic's OP-27 OP-amps and 170 metal film resistors.

The noise floor of the system was carefully checked with the spectrum analyzer and was just 6.75 nV/Hz which is equal to the quadrature sum of the two OP-27s at 3.8 nV/Hz and the Ithaco at 4.1 nV/Hz.

The end-to-end electronics gain of the two stages was measured by the transfer function capability of the 3582A spectrum analyzer and was tweaked where necessary to be within 1 percent of the gains stated on the front panel. All the data has been referred to the input through division by the gain numbers.

The worst-case signal-to-noise ratio occurs when the cans were present at 20 mA of drive current, $T = 300\text{K}$ and $f = .008\text{ Hz}$. At that limit, the SNR was 2-2. In all other cases,

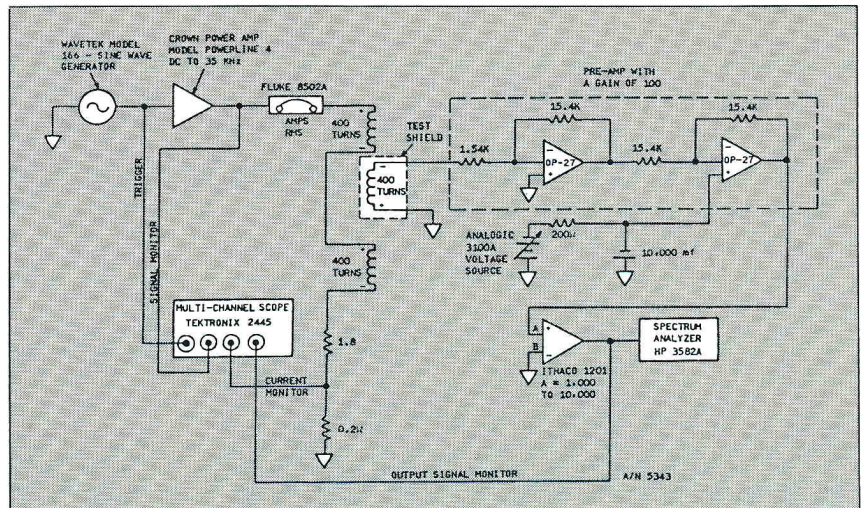
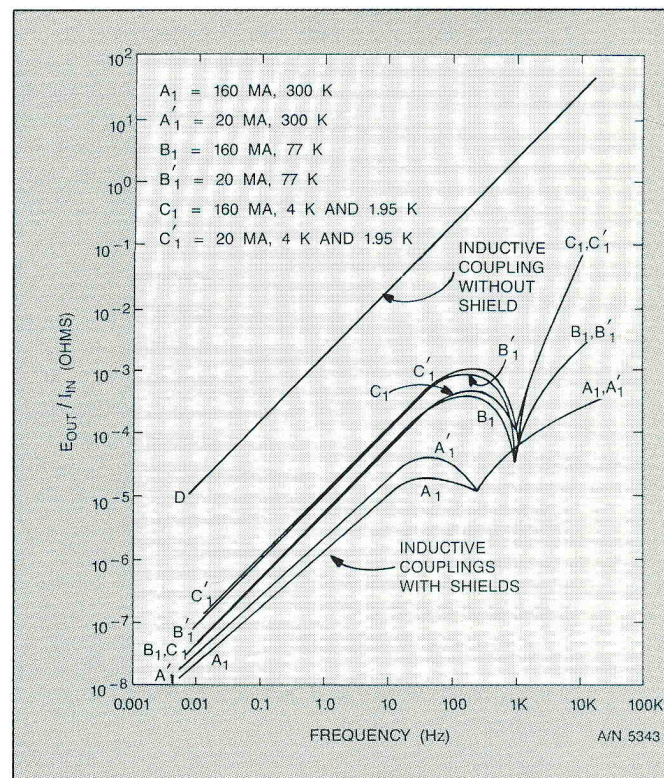


Figure 1.

the SNR was greater than 10 and frequently greater than 1,000.

The coils were hand-wound on a cardboard tube, 400 turns per coil and each coil was wound with standard No. 31 AWG insulated copper magnet wire.

The coils all had IDs of 4.5 cm and ODs of 5.5 cm. The internal pickup coil was left on its cardboard mandrel, and the mandrel was cut and shaped to provide a tight slip-fit transversely across the inside of the can. The outer two drive coils were removed from their mandrels and then tied into compressed circular coils with a winding thickness of .068 cm, while leaving the loop's ID and OD unchanged. The drive coils were connected in series-aiding and were aligned to be on axis with the pickup coil.



Figures 2 and 3. Curves A₁ through C₁' are raw data plots of E_{out}/I_{in} as shown in Figure 2. Curve D is the inductive coupling between them. Curve D is identical for all currents and tempera

Due to an overall diameter limitation set by the ID of the dewar neck (10.16 cm), the compressed outer coils were strapped hard against the outer wall of the can. They, in fact, were bent slightly to conform to the can's radius of curvature. Once the coils were in place on the cardboard model, each coil was adjusted by the removal of the few turns of wire to be 11 mH \pm 10 percent as measured in realtime on an HP LCRZ impedance meter. When added to the dewar cabling, the drive coils had a low Q resonance created by the stray capacitances associated with the coil winding and the cabling at 32 kHz.

The coupling between the coils was measured with the coils mounted on a close tolerance cardboard model of the cans. This kept the geometry of the three coils very closely the same both with and without the cans being present. The coils were mounted in the bottom third of the can to get as far away as possible from any field leaking out of the hole in the top or fringing from the small gap between the lid and the body.

Both sets of coils were connected to the 300k electronics through No. 28 AWG twisted shielded-pair cable, and the shields were all connected to a single-point ground. All ground loops were assiduously tracked down and dispatched.

The cans were supported by a very thin walled stainless steel tube being pushed through the hole in the lid. Just below the lid, we placed a small chip on the tube to prevent it from being extracted from the can. The can-coil assembly was positioned and held in place by tape.

The two sets of twisted shielded cables came down the inside of the tube. One cable went into the inside of the can and connected to the pickup coil. The other cable split out from the tube through a small notch cut in the side of the tube about 2 cm above the lid. The notch also let cryogenic fluids into, and vapor out of, the inside of the can.

Both cables came out of the top end of the tube and the top

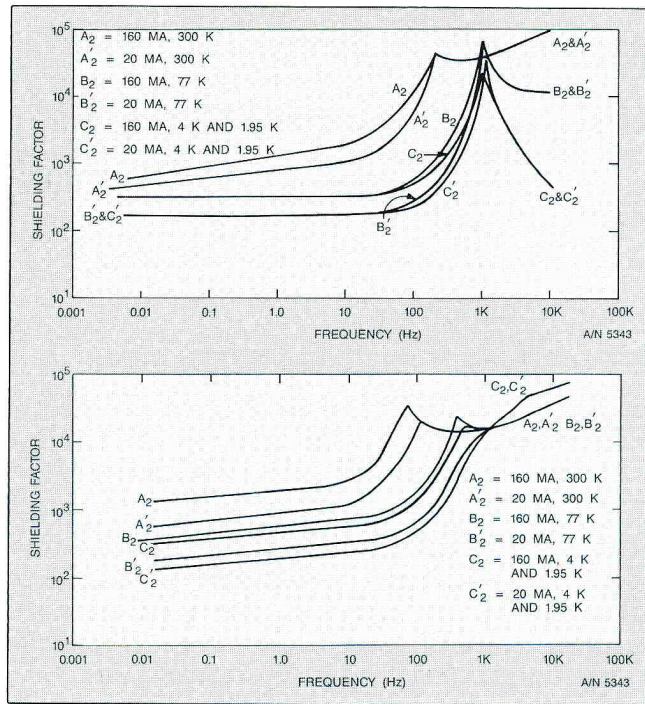


Figure 4 CPEXP-1184 Shielding Factor vs. Frequency, Temperature and Field. Figures 4 and 5 are plots of the shielding factor as a function of frequency. Curves A_2 through C_2' were obtained by dividing curve D in Figures 2 and 3 by the raw data curves A_1 through C_1' . The resulting set of curves represents the ratio of the inductive coupling between the input and output coils without shielding to the inductive coupling between the coils with shielding as a function of frequency, temperature and excitation field strength.

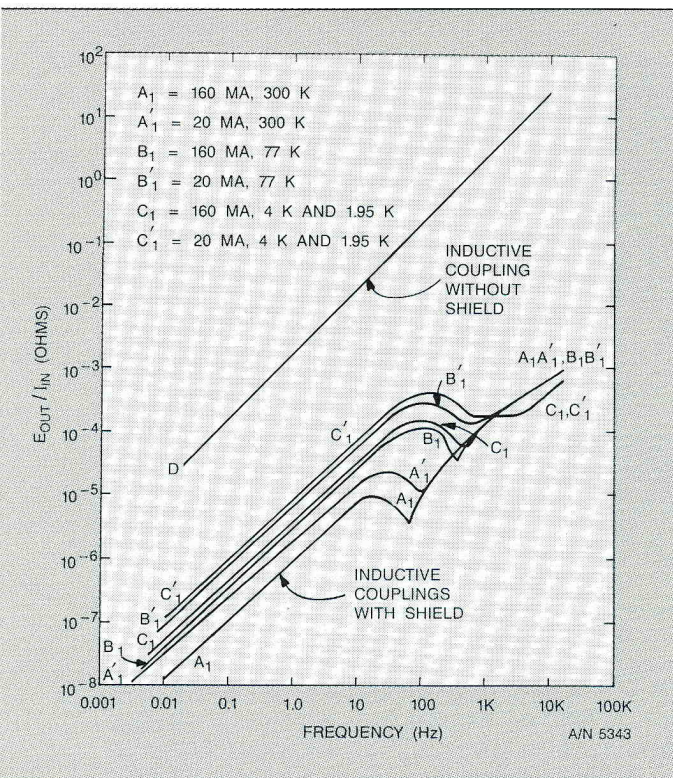
5 cm of the tube was sealed with an epoxy plug. This not only locked the cables in place at the top, but also sealed the tube so that the suspended unit would be pumped to superfluid pressures.

Data were taken on three runs, first on the cardboard model to get the baseline coupling data. All the data were taken inside the aluminum-walled, fiberglass necked dewar. Data at 300°K were taken first. Data were next taken at 77°, 4° and then 1.91°K. The temperature was taken from the saturated vapor pressure curves for LHe and pressure was monitored on a calibrated MKS Baratron head and readout. To lower the temperature from 4° to 1.91°K, the dewar volume was pumped through an auxiliary port with a 30 CFN rotary vane roughing pump. All low-temperature measurements were taken with the coils and then the coils with the can submerged in liquid; the liquid also filled the inside of the can.

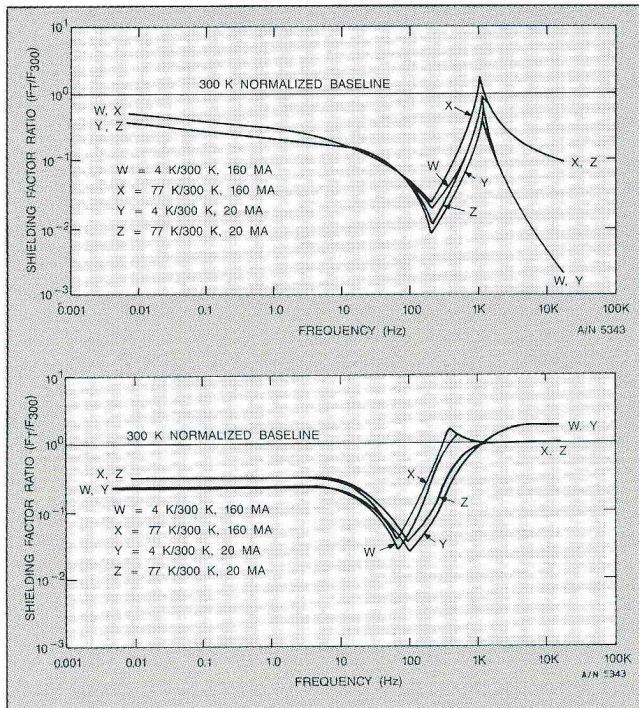
At all times, the coils were 11.5 cm from the nearest conductive wall, which we believe to preclude any eddy current effects in the dewar from affecting the data. We were also suspicious enough of the deep cusp at $f = 1$ kHz to check the coils and cans with the unit suspended in a large styrofoam cooler which we then filled with liquid nitrogen. During these tests, all extraneous conductive materials were at least 11.5 cm from the coils. The cusp remained unchanged during these retests.

Discussion of Results

The results of our study will not be discussed in great detail, this report being primarily a presentation of data. Arguments based on skin effects and domain wall motion can be made, however, allowing for a first-order understanding of the observed behavior. For a more comprehensive explanation



as a function of frequency with excitation currents and temperatures of the input and output coils as a function of frequency with no shielding and with shielding within the domain of interest.



Figures 6 and 7. Figures 6 and 7 represent the effect of temperature on the shielding factor ratio as a function of frequency, normalized to a 300°K baseline.

of ferromagnetic behavior, the reader is referred to the list of references at the end of the paper. Details of the annealing process, being one of a proprietary nature, are not discussed. Any differences in the shielding factor characteristics of the two specimens are assumed to be a function of the fabrication and annealing processes.

The behavior of the two cans as a function of temperature, frequency and excitation field strength is nearly identical below 1 kHz. The shielding factor of both materials is relatively constant as a function of frequency between .01 Hz and 10 Hz and increases by nearly two orders of magnitude between 1 Hz and 1 kHz. Divergent behavior in the shielding factor is observed in the AD-MU-78 sample above 1 kHz, with its 4°K shielding factor falling off by two orders of magnitude and its 300°K shielding factor improving slightly.

The CP-EXP-1184 can shows convergent behavior above 1 kHz with a marked improvement in the 4°K shielding over that at 300°K.

A slight field strength dependence is evidenced in both materials. Below 100 Hz, CP-EXP-1184 exhibits a field strength dependence throughout the entire temperature domain, whereas AD-MU-78 shows a field strength dependence only at 300°K. Between 100 Hz and 1 kHz, the primed and unprimed CP-EXP-1184 data curves converge, indicating a dramatic falloff in the field strength dependence of the shielding factor within this frequency band. A temperature-dependent translation of the point of convergence is observed with this point translated to higher frequencies at lower temperatures. All of the CP-EXP-1184 data curves intersect at 1 kHz with the 300°K and 77°K curves converging thereafter. The 77°K and 4°K shielding factors of AD-MU-78 are identical below 100 Hz. A slight temperature dependence within this temperature domain is evidenced between 100 Hz and 1 kHz, with a dramatic increase in the temperature dependence above 1 kHz.

The shielding factor curves show a crisp-like behavior between 100 Hz and 1 kHz, again attributed to skin effects, with a temperature dependent translation in the maximum shielding factor to higher frequencies. At frequencies above this critical value, the shielding factor is no longer dependent on the applied field strength.

Between 10 Hz and 100 Hz, both samples show an order of magnitude degradation in their shielding factor ratios. A minimum occurs at ~ 100 Hz for the CP-EXP-1184 sample and at ~ 200 Hz for AD-MU-78. Between 100 Hz and 1 kHz, an increase in the shielding factor ratio of almost two orders of magnitude was observed for both samples. Although the shielding factor ratio degrades between 10 Hz and 100 Hz, the shielding at all temperatures, for both samples, increases within this frequency band. It should be noted that, although both samples exhibit relatively stable shielding as a function of frequency between .01 Hz and 10 Hz, there is virtually no frequency dependence of the shielding factor ratio of the CP-EXP-1184 sample within this frequency range, although a slight linear decrease in the shielding factor ratio of AD-MU-78 is observed.

Summary

Many high permeable soft ferromagnetic materials can be bought commercially, however, very few are commercially available which exhibit effective shielding at cryogenic temperatures down to 4°K. AD-MU-78 and CP-EXP-1184 are of the same material composition, however, they have undergone separate and distinct processes. Although both sample materials exhibit similar behavior below 1 kHz, their behavior becomes quite divergent at frequencies above 1 kHz. Whereas AD-MU-78 degrades significantly in going from 300°K to 4°K at these high frequencies, the CP-EXP-1184 sample shows a marked improvement in its 4°K shielding factor over its

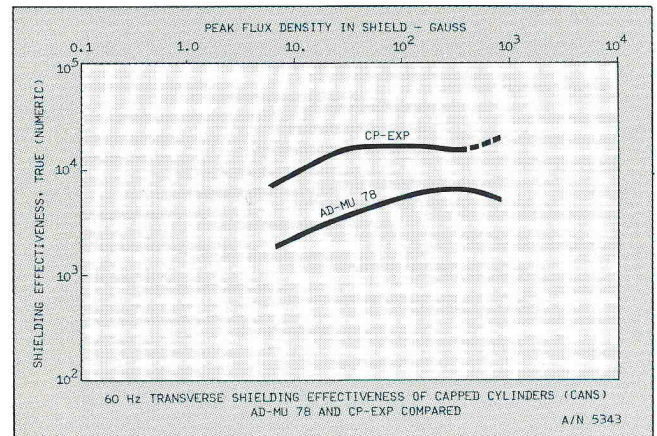


Figure 8. 60 Hz Transverse Shielding Effectiveness of Capped Cylinders (cans), AD-MV 78 and CP-EXP Compared.

shielding factor at 300°K.

It can be concluded that for shielding at low frequencies, both AD-MU-78 and CP-EXP-1184 exhibit effective and stable behavior as a function of temperature, however, for shielding at frequencies above 1 kHz, CP-EXP-1184 is a much better shield at cryogenic temperatures. Because of their shielding effectiveness at low temperatures, they would, therefore, be useful for localized cryogenically cooled magnetic shielding for such devices as sensitive magnetometers. **EE**